Geomechanics and Engineering, *Vol. 34, No. 1 (2023) 103-113*
https://doi.org/10.12989/gae.2023.34.1.103

TBM disc cutter ring type adaptability and rock-breaking efficiency: Numerical modeling and case study

Xiaokang Shao[1a], Yusheng Jiang*[1], Zongyuan Zhu[1b], Zhiyong Yang[1c], Zhenyong Wang[1d], Jinguo Cheng[1e] and Quanwei Liu[2f]

[1]*School of Mechanics and Civil Engineering, China University of Mining and Technology-Beijing, Ding, No. 11 Xueyuan Road, Haidian District, Beijing 100083, P.R. China*
[2]*Qingdao Metro Line 6 Co Ltd, No.177 Binhai Road, Huangdao District, Qingdao 266000, P.R. China*

(*Received November 16, 2022, Revised May 3, 2023, Accepted June 7, 2023*)

Abstract. This study focused on understanding the relationship between the design of a tunnel boring machine disc cutter ring and its rock-breaking efficiency, as well as the applicable conditions of different cutter ring types. The discrete element method was used to establish a numerical model of the rock-breaking process using disc cutters with different ring types to reveal the development of rock damage cracks and variation in cutter penetration load. The calculation results indicate that a sharp-edged (V-shaped) disc cutter penetrates a rock mass to a given depth with the lowest load, resulting in more intermediate cracks and few lateral cracks, which leads to difficulty in crack combination. Furthermore, the poor wear resistance of a conventional V-shaped cutter can lead to an exponential increase in the penetration load after cutter ring wear. In contrast, constant-cross-section (CCS) disc cutters have the highest quantity of crack extensions after penetrating rock, but also require the highest penetration loads. An arch-edged (U-shaped) disc cutter is more moderate than the aforementioned types with sufficient intermediate and lateral crack propagation after cutting into rock under a suitable penetration load. Additionally, we found that the cutter ring wedge angle and edge width heavily influence cutter rock-breaking efficiency and that a disc cutter with a 16 to 22 mm edge width and 20° to 30° wedge angle exhibits high performance. Compared to V-shaped and U-shaped cutters, the CCS cutter is more suitable for soft or medium-strength rocks, where the penetration load is relatively small. Additionally, two typical case studies were selected to verify that replacing a CCS cutter with a U-shaped or optimized V-shaped disc cutter can increase cutting efficiency when encountering hard rocks.

Keywords: blade width; cutter ring type; damage crack; discrete element method; rock breaking; TBM construction; wedge angle

1. Introduction

The widespread application of full-face tunnel boring machines (TBMs) has rapidly improved tunnel construction efficiency. Such TBMs have obvious advantages in terms of integrating driving, support, soil discharge, and construction material transportation systems, as well as advantages over traditional mine-tunneling methods in terms of engineering efficiency and safety (Chen *et al*. 2018). The disc cutter is the primary rock-breaking tool installed on the TBM cutterhead. It exerts thrust and rotational torque to allow the cutter to penetrate rock and roll on the tunnel face, causing rock damage. Under the reciprocating penetrating-cutting action of the disc cutter in each adjacent trajectory, the cracks in rock are connected and break through, causing the rock mass on the tunnel face to chip and fall off to realize rock breaking. However, the rock damage mechanisms and applicable conditions of different cutter rings are diverse. Therefore, studying the mechanical contact behavior between different types of disc cutters and rock is of great significance.

The ring-type design and layout of the disc cutter significantly affect the efficiency and cost of a project. Therefore, research on disc cutter design, layout, and tunneling efficiency is an important topic in TBM engineering. It has been found that blade width significantly impacts rock-breaking efficiency, particularly for extremely hard rocks (e.g., granite with a uniaxial compressive strength greater than 150 MPa), where a narrower blade width can often achieve higher efficiency (Ning *et al*. 2020). Research on disc cutter spacing, on the other hand, has shown that as the spacing increases, rock-breaking efficiency decreases, leading to the concept of optimal cutter spacing (Pan 2017). Additionally, significant work has focused on models for predicting disc cutter loads, including the extrusion-breaking model for V-shaped disc cutter penetration tests (Evans 1965, Roxborough and Phillips 1975, Wijk 1992), extrusion-shear breaking model (Farrokh *et al*. 2012, Ozdemir and Wang 1979), extrusion-

*Corresponding author, Professor
E-mail: yusheng.jiang@cumtb.edu.cn
[a]Ph.D. Student
[b]Master student
[c]Professor
[d]Ph.D. Student
[e]Ph.D. Student
[f]Professor

ISSN: 2005-307X (Print), 2092-6219 (Online)

tension breaking mode (Sanio 1985), and Colorado School of Mines model for linear cutting tests with a constant-cross-section (CCS) disc cutter (Rostami and Ozdemir 1993, Rostami *et al*. 1996, Rostami 1997). However, these studies have rarely involved the rock-breaking effectiveness, applicable conditions, and layout methods of cutters with different cross-sectional shapes. In particular, the influence of disc cutter cross-sectional shape on the determination of cutter spacing has received little attention.

In this study, a numerical model of a rock sample and disc cutter was established using the discrete element method to simulate the process of rock breaking by cutters with different ring shapes. Our goal is to reveal the influence of shape parameters such as cross-sectional shape, blade width, and wedge angle on the rock-breaking effect. By comparing the development processes of internal damage and fracture after different types of cutters penetrate a rock mass, applicable conditions and optimization methods for cutter shape parameters are obtained, which can provide a reference for the type selection and arrangement of TBM engineering cutters under different rock strata conditions.

The remainder of this paper is organized as follows. Section 2 describes the definitions of different cutter layouts and ring types. Section 3 describes our experimental methods and the considered material properties. Section 4 presents the results of our experiments and the analysis thereof. Section 5 presents some practical applications of our findings. Finally, Section 6 concludes this paper and summarizes our findings.

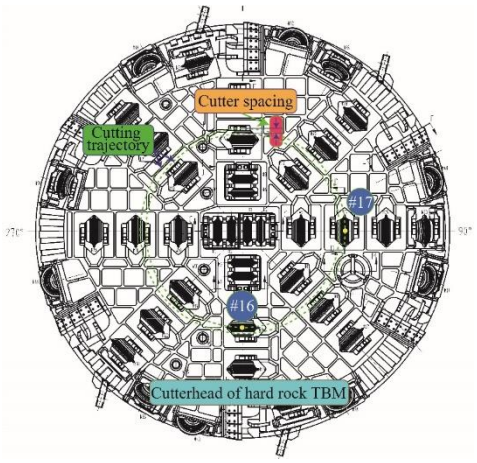

(a) TBM disc cutter layout

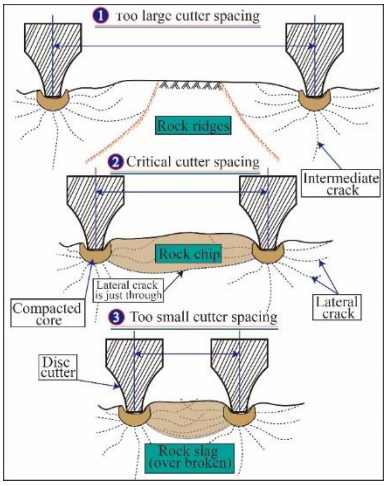

(b) Disc cutter spacing and rock-breaking effect

Fig. 1 Cutterhead configuration and cutter spacing settings

2. Cutter layout and ring type

The disc cutter on a TBM cutterhead is typically arranged according to the Archimedes helix. The distance between the adjacent trajectories of the disc cutter cutting on the tunnel face is defined as the cutter spacing (Li 2019), as shown in Fig. 1(a). In engineering practice, the disc cutter spacing is generally set to 50 to 100 mm and it increases as the disc cutter size increases. Cutter spacing is an essential parameter in TBM cutter design and significantly affects rock-breaking efficiency. As shown in Fig. 1(b), under the intrusion of the disc cutter, the rock stress in contact with the blade increases, and compression and shear damage occur. The rock under the cutter blade is crushed into powder to form a compacted core, which transfers the penetrating force to the surrounding rock and gradually initiates fine radial cracks around the core (She *et al*. 2022). When the cutter spacing is too large, the lateral cracks formed by adjacent cutters cannot be connected easily. Only the lateral cracks near the dense nucleus develop to the surface of the rock mass (tunnel face), causing the rock to chip and break away from the tunnel face. The rock mass in the middle area of the adjacent cutter tracks is not broken to form rock ridges, which prevents the cutter from advancing. In contrast, when the cutter spacing is too small, the rock cracks on adjacent tracks are closely crossed and stacked, and the rock mass in the middle is broken into small pieces, resulting in greater energy loss for rock breaking and poor rock-breaking efficiency (Tuncdemir *et al*. 2008). Therefore, only when the rock cracks under adjacent cutting trajectories just break through, meaning no rock ridges are formed, is the cutter spacing equal to the critical distance between adjacent cutters (Jing *et al*. 2018), which is also the threshold for cutter installation spacing on the cutterhead. An unfavorable scenario occurs when there are unbroken rock ridges between the rotation trajectories of adjacent cutters, which requires the cutter to roll and cut in grooves many times. In such a scenario, the rock-breaking efficiency is poor and cutter ring experiences significant wear.

Generally, disc cutter ring types can be divided into wedge and constant-cross (contains approximately CCS) types according to their cross-sectional shape and blade types include wedge (V-shaped), arc-edge (U-shaped), and flat-edge (CCS) types, as shown in Fig. 2 (Song *et al*. 2005). It is known that a wedge-type cutter requires the smallest penetrating load to break rock, but its blades are prone to curling or rapid wear, whereas the blade width of a CCS-type disc cutter remains almost unchanged after wear. The diameter, blade width (w), and wedge angle (θ) are important parameters for disc cutters and affect the rock-breaking efficiency and cutter layout (Sun *et al*. 2015).

Table 1 Calibration of microscopic parameters

Rocks	UCS (MPa)	P (GPa)	κ (-)	P_b (GPa)	κ^* (-)	τ (MPa)	C (MPa)	f (°)
Tuff	148	10	1	10	9	80	200	0.4
Granite	77	10	1	10	3	30	70	0.4

Note: UCS = uniaxial compressive strength; P = particle contact modulus; P_b = Parallel modulus of adhesion; κ = inter-particle normal-to-tangential stiffness ratio; κ^* = parallel-bonded normal-to-tangential stiffness ratio; τ = parallel bonding tensile strength; C = parallel bonding cohesion; f = parallel adhesion friction angle

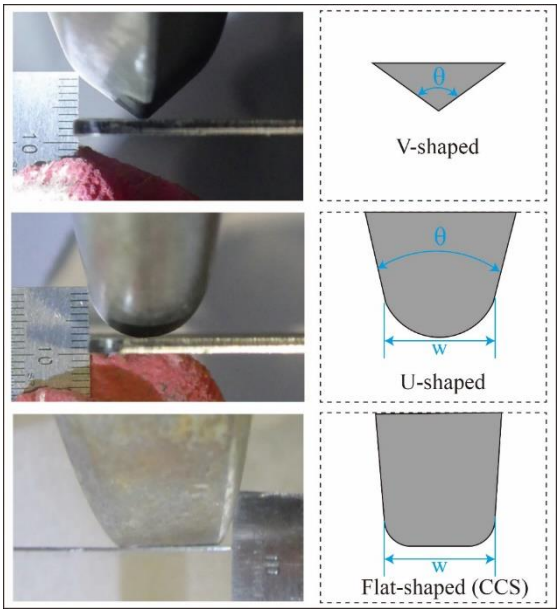

Fig. 2 Cross-section type of disc cutter blades (Chang *et al*. 2013)

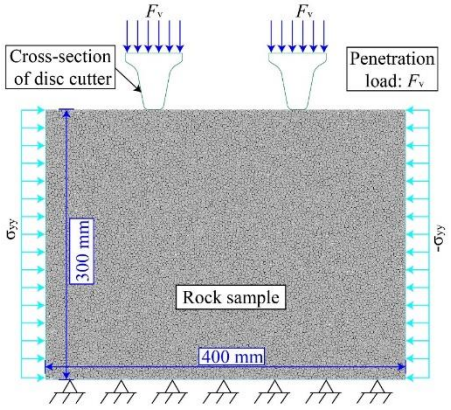

Fig. 3 Model used for numerical testing

3. Methods and material properties

To investigate the influence of the disc cutter ring type on rock-breaking efficiency, a numerical simulation testing method was adopted to establish a cutter-rock interaction model to simulate the rock-breaking process after adjacent disc cutters penetrate a rock mass.

3.1 Numerical modeling

The rock sample and disc cutter were modelled using the large-scale discrete element calculation software PFC. The rock was mimicked by "ball" particles and the disc cutter was constructed using "wall" elements. The contact between ball particles can be defined using adhesion parameters to reflect the physical and mechanical properties of rock, and wall elements can be given a specified motion state to simulate a disc cutter penetrating the rock. Limited by the calculation scale of the discrete element program, the size of the rock model was set to 400 ×300 mm, which was enough to overcome the influence of boundary effects. It contains two adjacent trajectories cutter models. And the disc cutter ring with a diameter of 19 inches (483 mm) was selected, which was commonly used in engineering practice, as shown in Fig. 3. Stress servo boundaries were used on both sides of the rock sample to simulate the surrounding pressure state of the rock on the tunnel face with a fixed boundary applied to the bottom of the sample to hold the model in place and a free surface at the top as the disc cutter penetrates.

3.2 Parameter calibration

The contact parameters between the ball particles of the rock sample can be specified to represent the mechanical characteristics of rock. The parallel bond model is the most commonly used model for mimicking rock materials (Xu *et al*. 2020, Li *et al*. 2022). The mechanical parameters assigned to the ball particles in numerical simulations need to be calibrated based on the macroscopic mechanical parameters of rock to ensure that a rock sample composed of ball particles has mechanical properties that approximate those of an actual rock mass (Zhou *et al*. 2017, Ren *et al*. 2017). Rock specimens were first cut into standard models for uniaxial compressive strength (UCS) testing to obtain their mechanical properties. Subsequently, the same specimen size and loading method were used for the numerical simulation of rock strength so that ball particles with acceptable mechanical parameters exhibited the same mechanical properties as actual rock specimens. The rock specimens used for testing were tuff and granite taken from the TBM tunnel of Qingdao Metro Line 6. The UCS test procedure is presented in Fig. 4, and the rock mechanical and numerical simulation parameters are listed in Table 1.

The contact key between the ball particles in linear parallel bond model has a specific stiffness to resist normal force, shear force, and torque. When the external force on the particles exceeds the bond strength threshold, a bond breaks and a microcrack is formed, as shown in Fig. 5. According to the type of bond fracture, cracks can be divided into tension and shear cracks, which can simulate fissures within the rock under disc cutter loads (Zhang *et al*. 2020).

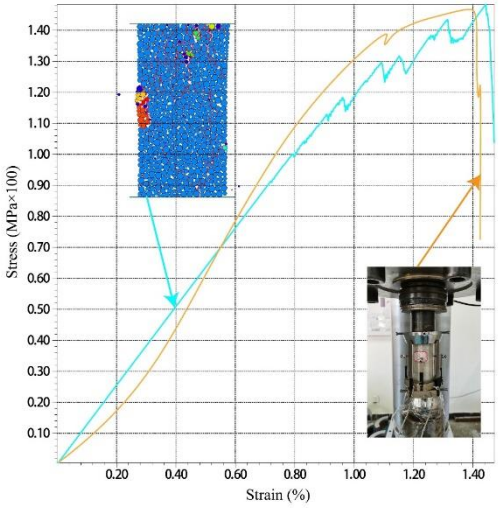

(a) Tuff specimens

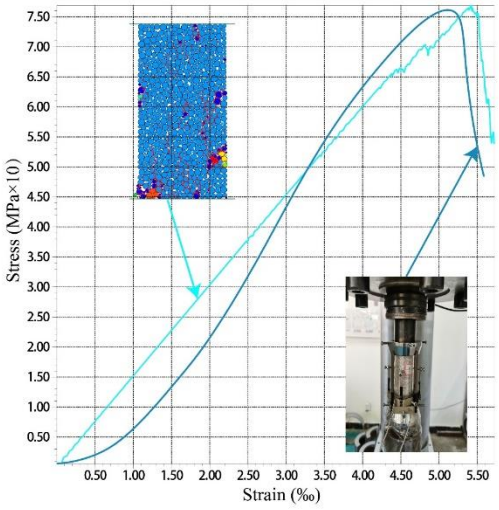

(b) Granite specimens

Fig.4 Strength testing and numerical simulation results of specimens

4. Results and analysis

4.1 Different ring types for disc cutters

Significant differences were observed in crack propagation within the rock under the penetration of disc cutters with different blades, as shown in Fig. 6. For the same depth of cutter penetration, the flat-shaped disc cutter provides the largest contact area with the rock surface. As a result, the rock under the flat-shaped cutter blade fractures and forms the broadest range of compact cores. The cracks in the compact core are mainly tensile with few shear cracks. As shown in Fig. 6(b), the cracks at the bottom of the core develop farther into the rock to form intermediate cracks, which are long and widely distributed. In contrast, the compacted cores at the two corners of the cross-section of the cutter develop lateral cracks outwards, resulting in radial cracking. As shown in Fig. 6(c), the range of the compacted core and number of total cracks inside the rock formed by the intrusion of the V-shaped disc

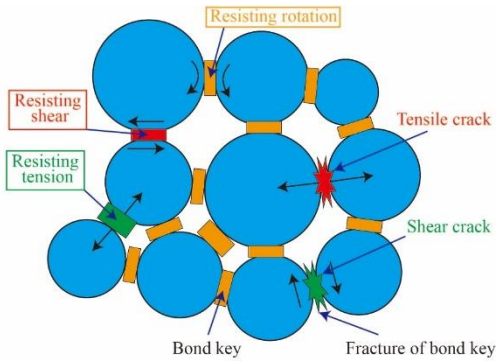

Fig.5 Parallel bond model and particle microcracks

cutter are both the smallest and are principally tensile. The major fractures inside the rock are few, but they are always long. It can be concluded that the penetration load transfer of the V-shaped cutter is the most concentrated, so the rock mass is broken into relatively large rock chips. Regarding the number of cracks and extent of the crack concentration, the U-shaped cutter combines the advantages of both the V-shaped and flat-shaped cutters. The intermediate cracks at the bottom are long and the lateral cracks on the side are concentrated and developed (Fig. 6(d)).

In terms of breaking efficiency, under the same disc cutter load, the V-shaped cutter is more prone to intrude into the rock, followed by the U-shaped cutter and flat-shaped cutter, which has the shallowest intrusion depth. The rock fissures under the flat-shaped cutter are the most developed, but are more dispersed, which makes it difficult to form long, penetrating fissures, resulting in low breaking efficiency. Particularly in hard rock, flat-shaped disc cutters have difficulty achieving the expected penetration, meaning wedge-shaped cutters with pointed or curved edges are more suitable.

The normal forces of the disc cutters during penetration are presented in Fig. 7(a) and the average normal forces for the flat-shapes, U-shaped, and V-shaped disc cutters are 209, 116, and 39 kN, respectively. These differences in cutter force reflect the difficulty of rock penetration for different blade types. Although the load required to intrude into the rock for a V-shaped disc cutter is much lower than that for a flat-shaped disc cutter, the wear resistance of a V-shaped disc cutter is much lower than that of a flat-shaped disc cutter and cutter rock-breaking efficiency is significantly reduced when a blade wears (Tumac *et al.* 2015). As shown in Fig. 7(b), the difficulty of intruding into the rock mass increases significantly as the V-shaped disc cutter wears and the required disc cutter normal force increases exponentially with the amount of wear as follows:

$$F_V=50\cdot e^{0.148\delta}, \quad (1)$$

$$R^2=0.85 \quad (2)$$

where F_v is the normal force of the disc cutter, δ is the extent of disc cutter wear, and R^2 is the fit goodness.

4.2 Disc cutter wedge angle

A U-shaped cutter is typically designed with a wedge

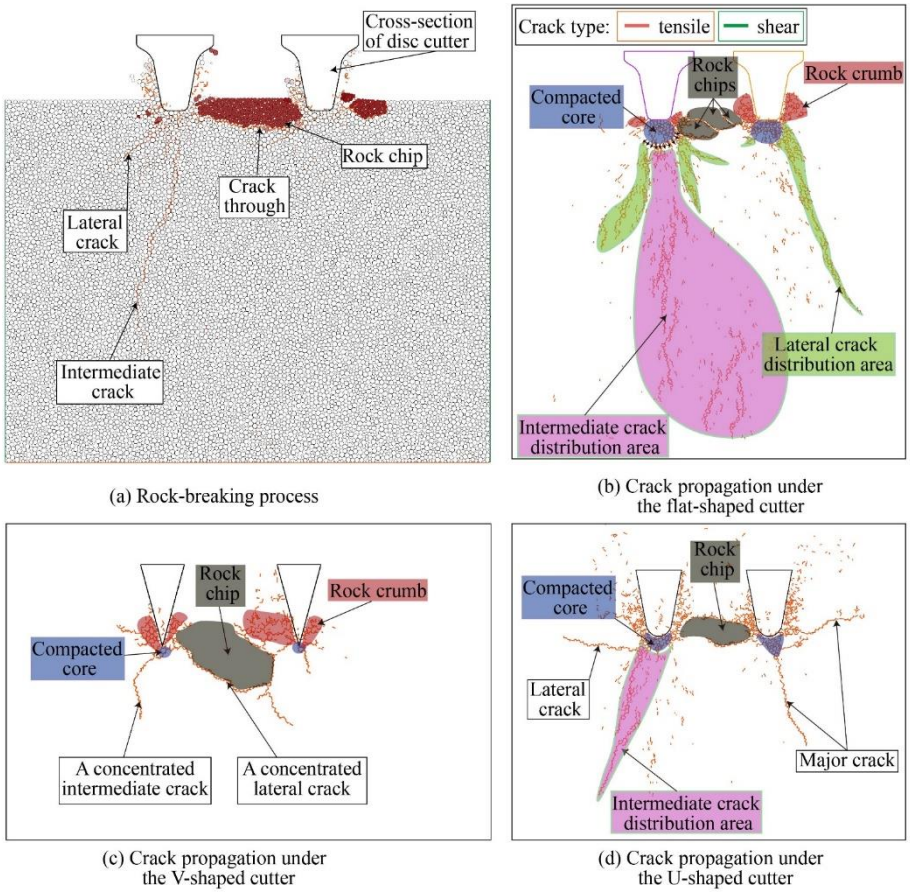

(a) Rock-breaking process

(b) Crack propagation under the flat-shaped cutter

(c) Crack propagation under the V-shaped cutter

(d) Crack propagation under the U-shaped cutter

Fig. 6 Development processes of rock fractures under different cutters

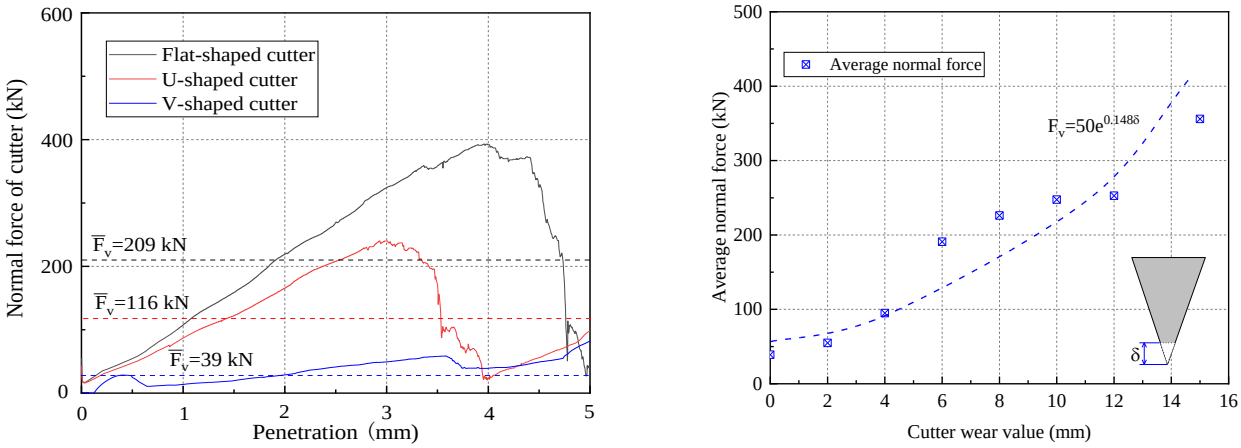

(a) Normal force curves for different types of cutters

(b) Cutter wear-force curve for a V-shaped disc cutter

Fig. 7 Cutter force curves with variations in penetration and the cutter wear value

angle (θ) such that it requires less normal force when penetrating rock compared to a flat-shaped cutter. Additionally, the cross-section of a U-shaped cutter ring remains approximately constant after wear, so its rock-breaking efficiency is relatively stable. Therefore, U-shaped cutters are widely used in hard-rock TBM engineering (Gou *et al.* 2022). The development of rock fractures under the penetration of a U-shaped cutter with different wedge angles is presented in Figs. 8(a) to 8(f). As the wedge angle increases, the range of the compacted cores below the blade increases, and the number and length of intermediate cracks remain essentially unchanged. However, the expansion of lateral fractures is promoted (Su *et al.* 2009). As shown in Fig. 8(g), as the wedge angle increases, the average normal force of the cutter and total number of cracks increase. To evaluate the rock-breaking efficiency of a disc cutter with different wedge angles, an important indicator (ΔF) is defined as the ratio of the average normal force ($\overline{F}_V$) to the total number of cracks (n) as follows

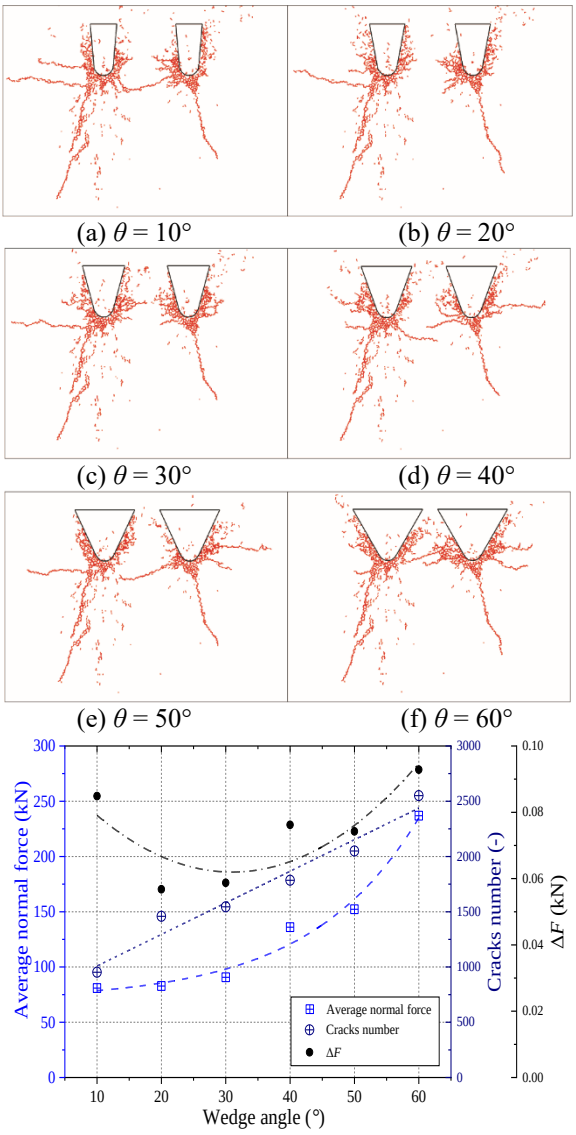

(g) Curves of cutter force and crack number

Fig. 8 Rock-breaking loads and crack development processes of cutters with different wedge angles

$$\Delta F = \frac{\overline{F}_V}{n}, \tag{3}$$

$$\overline{F}_V = 56.097e^{0.0217\theta} \tag{4}$$

$$n = 28.58\theta + 723.53 \tag{5}$$

$$\Delta F = 4\times10^{-05}\theta^2 - 0.0024\theta + 0.0993 \tag{6}$$

According to Fig. 8(g), ΔF first decreases and then increases with an increase in the wedge angle and the smaller value of ΔF, the higher the rock-breaking efficiency. It can be concluded that a wedge angle in the range of 20° to 30° has relatively high rock-breaking efficiency.

4.3 Blade width of a disc cutter

Blade width determines the direct contact area between the disc cutter and rock surface. The wider the blade, the more fractured the rock mass beneath the blade. Furthermore, a wider blade increases the normal disc cutter force required to achieve the same penetration. Therefore, selecting a suitable blade width is a critical parameter in cutter design in engineering practice. The radial wear on a disc cutter is typically measured in TBM engineering to reflect the wear extent and is an important criterion for determining whether to replace cutters. However, disc cutter wear is not only reflected by a reduction in disc cutter height (diameter), but also in a reduction in blade width, as shown in Fig. 9. When the disc cutter width is reduced, the rock-breaking capacity and work efficiency also decrease. Therefore, when servicing a cutterhead, attention should be devoted to the loss in the height and width of the blade simultaneously.

Fig. 9 Different wear forms of disc cutters

To study the effects of blade width (w) on wear efficiency, disc cutters with different blade widths were selected for rock-breaking tests. The fracture distributions of rock under disc cutters with different blade widths are presented in Fig. 10. When the blade width was no greater than 22 mm, the middle fractures below the compacted cores are more concentrated and appear as long and thin fractures. When the blade width exceeds 22 mm, a large number of scattered short fractures occur at the bottom of the rock. The number of lateral cracks is positively correlated with the blade width. Therefore, increasing the blade width is beneficial for the development of lateral cracks and promotes crack penetration and the completion of rock breaking under adjacent disc cutter loads. However, increasing the disc cutter width also reduces the penetration into the rock under the same disc cutter load, thereby reducing breaking efficiency. Therefore, as long as the cutter reaches a sufficient penetration depth under the rated cutter load, the blade width should be increased as much as possible to improve rock-breaking efficiency.

The normal forces of disc cutters with different blade widths during rock breaking are presented in Fig. 11. The correlation between the blade width with the cutter load and the number of cracks is as follows

$$\overline{F}_V = -0.1528\, w^2 + 18.876\, w - 91.378, \tag{7}$$

$$n = -4.6214\, w^2 + 312.1w - 1900.4 \tag{8}$$

When the blade width of the disc cutter is less than 12 mm, although the load required to break the rock is small, the number of fissures formed inside the rock is too small

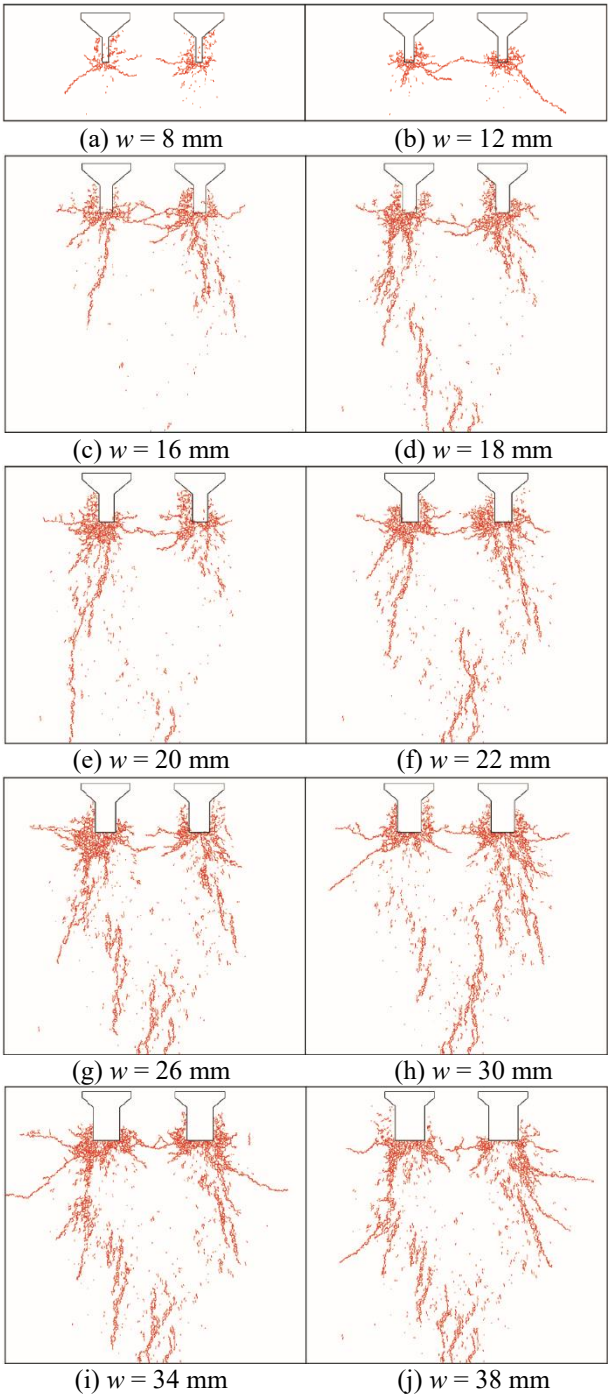

Fig. 10 Crack development under cutter penetration with different blade widths

and the ΔF value was high, resulting in poor breaking efficiency. When the blade width is increased to 16 mm, the normal force of the cutter and total number of cracks increase significantly and the rock-breaking efficiency is improved. Increasing the blade width to over 22 mm results in a minor increase in the number of fractures in the rock and requires a higher disc cutter load to achieve optimal breaking efficiency. Therefore, the use of 16 to 22 mm blade widths in harder rock optimizes the tradeoff between disc cutter penetration and breaking efficiency.

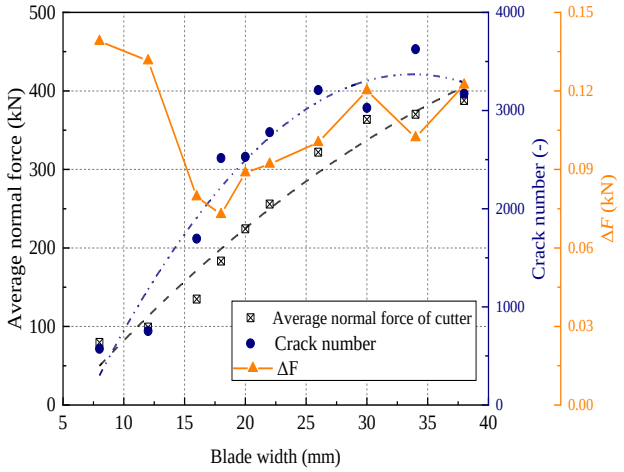

Fig. 11 Curves of force and crack number under cutters with different blade widths

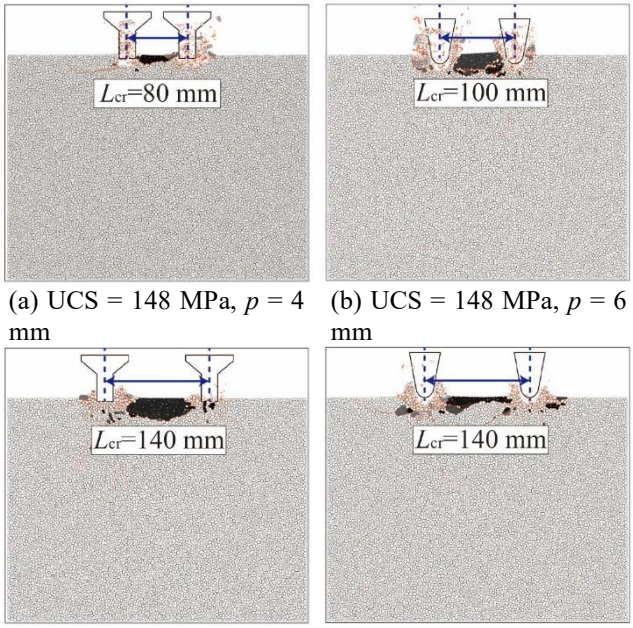

(a) UCS = 148 MPa, p = 4 mm (b) UCS = 148 MPa, p = 6 mm

(c) UCS = 77 MPa, p = 5 mm (d) UCS = 77 MPa, p = 7.5 mm

Fig. 12 Critical cutter spacing for flat-shaped and U-shaped cutters

4.4 Critical cutter spacing

Cutter spacing is an important parameter for evaluating the suitability of a cutter layout. In engineering applications, a cutter is typically replaceable and the cutter spacing is fixed. Therefore, an unreasonable cutter spacing reduces the rock-breaking efficiency of a cutterhead and such adverse conditions are difficult to improve after cutterhead manufacture. The determination of a reasonable cutter spacing is influenced by several factors, including rock strength, cutter size, and ring type. Most studies and adopt a method of establishing the ratio of cutter spacing to penetration to determine a reasonable range of cutter spacing, meaning they calculate cutter spacing according to a specific penetration rate. However, there are significant differences in the fracture development patterns of

the different disc cutter types after intrusion into rock. Therefore, a distinction should be made between different disc cutter ring types when determining cutter spacing. As shown in Fig. 12, when penetrating hard rock (e.g., UCS = 148 MPa), the penetration depth (p) of the flat-shaped disc cutter is 4 mm under the maximum rated cutter load (F_v = 280 kN) and the critical cutter spacing (L_{cr}) is only 80 mm, whereas the maximum penetration depth of the U-shaped disc cutter is 6 mm and the critical cutter spacing is 100 mm. When cutting softer rock (e.g., UCS = 77 MPa), the cutter penetration depth increases, rock cracks propagate more easily, and the critical cutter spacing of these two types of cutters can reach 140 mm. Therefore, when a TBM encounters a hard rock layer that makes it difficult to advance a flat-shaped disc cutter and the total thrust of the TBM cannot be increased again or the load per cutter is close to the limit bearing value of the shaft, the cutter ring type can be replaced with a U-shaped or V-shaped ring to increase tunneling efficiency. Conversely, in medium-strength or soft rock, a flat-shaped disc cutter typically provides greater efficiency.

5. Practical applications

5.1 Case study 1: TBM tunneling in hard-rock stratum

5.1.1 Project overview

Qingdao Metro Line 6 is an underground tunneling project under construction in Qingdao, Shandong Province, China. The total length of the line is approximately 30 km and the length of the tunnel constructed by a TBM is approximately 23 km. Line tunnels traverse complex and variable stratigraphic conditions, including hard rock, soil-rock composite strata, and soil layers such as gravel and sand. The tunnel interval from Qiantangjianglu Station to Binhaixueyuan Station is part of Qingdao Metro Line 6 and was constructed using a hard-rock TBM with a single-line boring length of approximately 1,150 m and tunnel vault burial depth of approximately 20.4 to 30.7 m. The tunnel mainly traverses slightly weathered granite and the saturated UCS of the rock was 45 to 155 MPa according to a preliminary survey.

5.1.2 TBM configuration parameters

The TBM configuration parameters are listed in Table 2. The cutterhead face was equipped with 20 19-inch disc cutters and two types of cutter rings were prepared to handle rock strength variations. The first was a flat-shaped cutter ring with a blade width of 22 mm and wedge angle of 20°, which was configured on the original cutterhead. The second type used U-shaped blades with a smaller blade width (19 mm) that could be installed when the original cutter had difficulty advancing through hard rock. The rings of the two cutters are machined by H13 tool steel with a Rockwell hardness value (HRC) of 58. The cutterhead layout and cutter cross-sectional design are illustrated in Fig. 13.

Table 2 TBM parameter table

Configuration	Parameters
Excavation diameter	6300 mm
Face cutter (number/diameter)	20 pcs/19 inches
Central cutter (number/diameter)	4 pcs/19 inches
Gauge cutter (number/diameter)	13 pcs/19 inches
Rated torque	2940 kN·m
Breakaway torque	5700 kN·m
Maximum total thrust	24150 kN

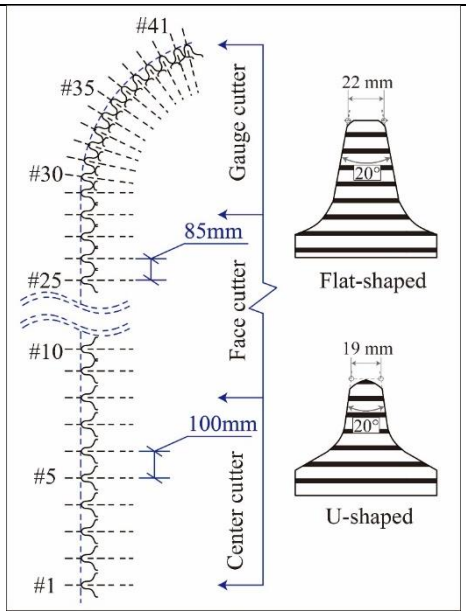

Fig.13 Cutter layout

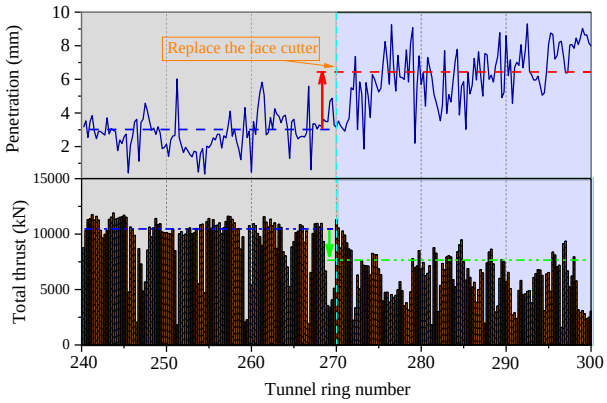

Fig. 14 Total thrust and penetration of a TBM before and after tool replacement

5.1.3 Tunneling parameters

The tunneling speed of the No. 240 to 270 rings was low with an average total thrust of over 10000 kN and average penetration of 3 mm/r. The discharge of rock slag was mostly rock detritus. Therefore, project managers attempted to replace the face cutter ring type with a U-shaped cutter to improve excavation efficiency. After cutter exchange, the average penetration rate of the No. 270 to 300 rings increased to 6 mm/r and the average total thrust decreased. The curves of the TBM total thrust and penetration rate before and after cutter exchange are presented in Fig. 14. In addition, by observing the shape of rock slag, it can be found that the side length of

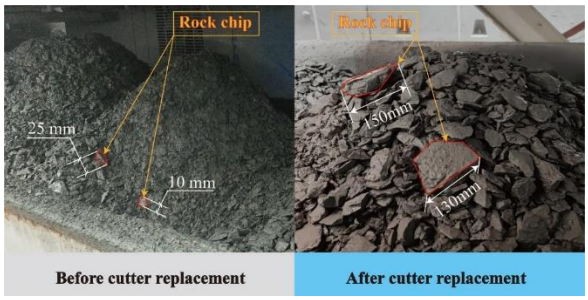

Fig. 15 Discharged rock chips before and after cutter replacement

Table 3 EPB-type TBM parameters

Configuration	Parameters
Excavation diameter	6303 mm
Face cutter (number/diameter)	22 pcs/18 inches
Central cutter (number/diameter)	6 pcs/17 inches
Gauge cutter (number/diameter)	12 pcs/18 inches
Rated torque	6000 kN·m
Breakaway torque	7200 kN·m
Maximum total thrust	39000 kN

rock chips is distributed mainly by 50~150 mm, which reflects that the cutterhead of TBM is in good working efficiency, as Fig. 15 shows. These results demonstrate that it is feasible and practical to improve tunneling efficiency by exchanging the cutter type on a TBM during excavation.

5.2 Case study 2: TBM encounter with super hard rock

5.2.1 Project overview

Qingdao Metro Line 6 from Chaoyanglu Station to Qiantangjianglu Station, which has a total line length of 4.74 km, was constructed using a composite earth pressure balance (EPB)-type TBM. The stratum from top to bottom consisted of vegetal fill, coarse sand, chalky clay, coarse sand, highly weathered tuff, medium-weathered tuff, and slightly weathered tuff. The tunnel was excavated at a depth of 12.8 to 31.6 m, mainly through the slightly weathered tuff, and the initial geological exploration revealed that the UCS of the surrounding rock was approximately 32.1 to 163.2 MPa.

5.2.2 TBM configuration parameters

Based on the presence of some fracture zones and composite strata in the tunnel area, it was difficult for the hard-rock TBM to ensure the stability of the tunnel face. Therefore, an EPB shield was used for tunneling with the configuration parameters listed in Table 3. The cutterhead was equipped with 22 18-inch face cutters. Because the cutterhead rotation speed of an EPB shield is much lower than that of a hard-rock TBM, the tunneling speed of the former is much lower than that of the latter in hard rock.

5.2.3 Tunneling parameters

During the actual construction of this tunnel section, a small section of super hard rock was encountered, which was

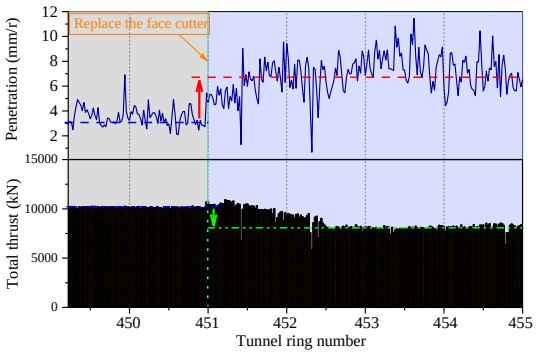

Fig. 16 Total thrust and penetration rate before and after cutter replacement

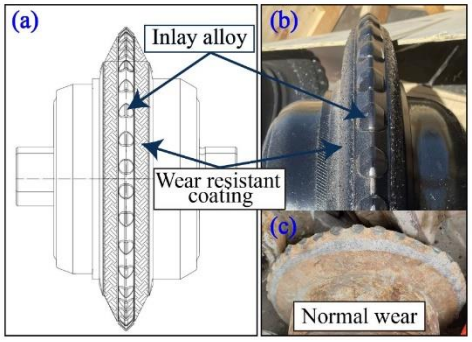

Fig. 17 Optimized V-shaped disc cutter: (a) design, (b) cutter photographs, and (c) cutter after tunneling

not revealed by geological exploration and was difficult to avoid. Based on the first stage of tunneling parameters shown in Fig. 16 (left), one can see that the average penetration rate of the cutterhead is only 3 mm/r and the tunneling time for each ring is as long as five hours. In full-face hard rock, the EPB shield can adopt the "empty chamber" mode or remain close to the empty state for tunneling. Therefore, it is very convenient to open the soil chamber for sampling. The measured maximum UCS of the rock on the tunnel face was as high as 170 MPa, which poses a significant challenge to EPB shield performance. To improve tunneling efficiency, the chamber was opened and the face cutter was exchanged before tunneling the 451st ring. Although a V-shaped disc cutter can penetrate rock to a sufficient depth under lower loads, its poor wear resistance makes it difficult to maintain rock-breaking efficiency. Therefore, in the practical application of this project, a conventional V-shaped disc cutter was improved to enhance the hardness and wear resistance of the cutting edge. As shown in Fig. 17, the disc cutter has a wedge cross-section and a high-hardness alloy material is laid along the blade ring to strengthen its rock-breaking ability. Additionally, both sides of the blade are covered with a wear-resistant material, i.e., tungsten carbide, which significantly enhances wear resistance and guarantees rock-breaking efficiency. The boring parameters after installed the V-shaped disc cutter are presented in Fig. 16, where the average penetration rate is increased to 6 mm/r and the total thrust required is reduced.

The wear resistance of the V-shaped disc cutter was also significantly improved. The cutter ring wear was normal and no alloy block chipping or cutter ring cracking was observed after tunneling (as shown in Fig. 17(c)).

6. Conclusions

In this paper, a rock-breaking test model for a disc cutter was established based on the discrete element method and used to simulate the propagation and distribution of cracks during the processes of different ring-type cutters penetrating rock samples. Based on the developed model, we were able to understand the influence of the cutter type on rock-breaking efficiency and the applicable conditions of different cutters, and the following conclusions can be drawn.

• The numerical simulation test results revealed the development process and distribution characteristics of fractures in a rock mass under the penetration of different types of cutters. The results indicated that most of the cracks in compacted cores were tensile cracks with a few shear cracks. When a flat-shaped cutter is adopted, the compacted core area is the largest, intermediate cracks are long, and the distribution range is relatively dispersed. In contrast, when a cutter with a V-shaped blade is used, the number of damage cracks in the rock mass is the lowest and cracks tend to concentrate and develop into long intermediate cracks. The number of cracks under the action of a U-shaped cutter is less than that under a flat-shaped cutter. However, intermediate and lateral cracks are relatively concentrated.

• Due to the difference in the critical cutter spacing applicable to disc cutters with different ring types, the strength of the rock formation should be fully considered to select the size and blade shape of the disc cutter first at the beginning of designing the cutterhead and then determined cutter spacing. The cutter forces during rock breaking with different blade types revealed that a flat-shaped disc cutter requires the highest load, and a V-shaped disc cutter requires the lowest load at the same penetration depth. Additionally, the wear resistance of a V-shaped cutter is poor and disc cutter load increases exponentially with wear according to the formula of $F_V=50\cdot e^{0.148\delta}$.

• The cutter wedge angle affects the expansion of lateral fractures and cutter force at the same penetration depth. We defined the average cutter normal stress ratio to the total rock crack number as ΔF, which can be used to assess cutter efficiency effectively. Furthermore, our analysis results indicate that a cutter with a wedge angle of 20° to 30° always has a high rock-breaking efficiency. The blade width directly affects the number of rock damage cracks and required level of penetration load. In hard rock, selecting a blade width of 16 to 22 mm can ensure a suitable penetration rate and high rock-breaking efficiency, whereas in soft rock, the energy consumption ratio of tunneling can be reduced by increasing the blade width or cutter spacing. Additionally, two case studies on typical engineering cases proved that tunneling efficiency can be significantly improved by changing the type of cutter ring when a TBM encounters harder rock and the cutter spacing or other machine design parameters cannot be changed.

Acknowledgments

This study was financially supported by the National Natural Science Foundation of China (Grant No. U1261212). The authors would also like to acknowledge the support provided by the China Railway First Group and China Railway Tunnel Group.

References

Chang, S.H., Choi, S.W., Park, Y.T., Lee, G.P. and Bae, G.J. (2013), "Experimental evaluation of the effects of cutting ring shape on cutter acting forces in a hard rock", *J. Korean Tunn. Undergr. Space Asso.*, **15**(3), 225-235. https://doi.org/10.9711/KTAJ.2013.15.3.225.

Chen, K., Sun, Z.C. and Li, T. (2018), *TBM Design and Construction*, China Communications Press Co., Ltd., Beijing, China.

Evans, I. (1965), "The force required to cut coal with blunt wedges", *Int. J. Rock Mech. Min. Sci. Geomech. Abstr.*, **2**(1), 1-12. https://doi.org/10.1016/0148-9062(65)90018-5.

Farrokh, E., Rostami, J. and Laughton, C. (2012), "Study of various models for estimation of penetration rate of hard rock TBMs", *Tunn. Undergr. Sp. Tech.*, **30**, 110-123. https://doi.org/10.1016/j.tust.2012.02.012.

Gou, B., Duan, W.J., Mo, J.L. and Zhang, M.Q. (2022), "Effects of TBM cutter profile on cutter-rock contact and damage behavior", *J. Chongqing Univ. Techno.* (*Natural Science*).

Jing, L.J., Zhang, N., Yang, C. and Ju, X.Y. (2018), "A design method research on TBM face cutter spacing layout based on minimum specific energy", *J. China Rail. Soc.*, **40**(12), 123-129.

Li, J.B. (2019) *TBM Structure and Application*, China Communications Press Co., Ltd., Beijing, China.

Li, T., Chen, G.B. and Li, Q.H. (2022), "Experimental study on rock-coal-rock composite structure with different crack characteristics", *Geomech. Eng.*, **29**(4), 377-390. https://doi.org/10.12989/gae.2022.29.4.377.

Ning, B., Xia, Y., Lin, L., Zhang, X., He, Y. and Liu, Y. (2020), "Experimental study on the adaptability of cutters with different blade widths under hard rock and extremely hard rock conditions", *Acta Geotech.*, **15**(11), 3283-3294. https://doi.org/10.1007/s11440-020-00958-0.

Ozdemir, L. and Wang, F.D. (1979), "Mechanical tunnel boring prediction and machine design", *Nasa Sti/recon Techni. Repo. N*, **80**, 16239.

Pan, Y.C. (2017), "Experimental study on rock cutting mechanism by TBM disc cutter for different rock strengths and confining stresses", Ph.D. Dissertation, University of Chinese Academy of Sciences, Beijing.

Ren, Z.Y., Pan, W.D., Liu, S.M. and Zhou, S. (2017), "Numerical simulation of non-parallel double crack propagation and coalescence in rock specimen", *J. Min. Sci. Technol.*, **2**(1), 33-41.

Rostami, J. (1997), "Development of a force estimation model for rock fragmentation with disc cutters through theoretical modeling and physical measurement of crushed zone pressure", Ph.D. Dissertation, Colorado School of Mines, Colorado.

Rostami, J., Ozdemir, L. and Nilson, B. (1996), "Comparison between CSM and NTH hard rock TBM performance prediction models", *Proceedings of the Annual Technical Meeting of the Institute of Shaft Drilling Technology*, Las Vegas, May.

Rostami. J. and Ozdemir, L. (1993), "New model for performance production of hard rock TBMs", *Proceedings of the Rapid Excavation and Tunneling Conference*.

Roxborough, F.F. and Phillips, H.R. (1975), "Rock excavation by disc cutter", *Int. J. Rock Mech. Min. Sci. Geomech. Abstr.*, **12**(12), 361-366.

Sanio, H.P. (1985), "Prediction of the performance of disc cutters in anisotropic rock", *Int. J. Rock Mech. Min. Sci. Geomech. Abstr*., **22**(3), 153-161.

She, L., Zhang, S.R., He S.W., Wang, C., Li, L., Jing, Y. and Liu, Y. (2022), "Investigation on wear prediction model of TBM disc cutter based on dense core theory", *Chinese J. Geotech. Eng*., **44**(5), 970-978.

Song, K.Z., Yuan, D.J. and Wang, M.S. (2005), "Study review on the interaction between disk cutter and rock", *J. Rail. Eng. Soc*., **6**, 66-69.

Su, L.J., Sun, J.S. and Lu, W.B. (2009), "Research on numerical simulation of rock fragmentation by TBM cutters using particle flow method", *Rock Soil Mech*., **30**(9), 2823-2829.

Sun, W., Guo, L., Zhou, J.J. and Huo, J.Z. (2015), "Rock fragmentation simulation under dual TBM disc cutter and design of cutter ring", *J. China Coal Soc*., **40**(6), 1297-1302.

Tumac, D. and Balci, C. (2015), "Investigations into the cutting characteristics of CCS type disc cutters and the comparison between experimental, theoretical and empirical force estimations", *Tunn. Undergr. Sp. Tech.*, **45**(1), 84-98. https://doi.org/10.1016/j.tust.2014.09.009.

Tuncdemir, H., Bilgin, N., Copur, H. and Balci, C. (2008), "Control of rock cutting efficiency by muck size", *Int. J. Rock Mech. Mini. Sci*., **45**(2), 278-288. https://doi.org/10.1016/j.ijrmms.2007.04.010.

Wijk, G. (1992), "A model of tunnel boring machine performance", *Geotech. Geol. Eng*., **10**(1), 19-40. https://doi.org/10.1007/BF00881969.

Xu, Z.H., Wang, W.Y., Lin, P., Xiong, Y., Liu, Z.Y. and He, S.J. (2020), "A parameter calibration method for PFC simulation: Development and a case study of limestone", *Geomech. Eng*., **22**(1), 97-108. https://doi.org/10.12989/gae.2020.22.1.097.

Zhang, Z., Zhang, K., Dong, W. and Zhang, B. (2020), "Study of rock-cutting process by disc cutters in mixed ground based on three-dimensional particle flow model", *Rock Mech. Rock Eng*., **53**(8), 3485-3506. https://doi.org/10.1007/s00603-020-02118-y.

Zhou, T.B., Yang, X.B. and Han, X.X. (2017), "Numerical inversion simulation of coal and rock under uniaxial compression failure in PFC2D", *J. Min. Sci. Techno*., **2**(3), 260-266.

GC